

## Bond strength and computational analysis for silane coupling treatments on the adhesion of resin block for CAD/CAM crowns

Kou TSUKAGOSHI, Masatsugu HIROTA, Rie NOMOTO and Tohru HAYAKAWA

Department of Dental Engineering, Tsurumi University School of Dental Medicine, 2-1-3 Tsurumi, Tsurumi-ku, Yokohama, Kanagawa 230-8501, Japan

Corresponding author, Masatsugu HIROTA; E-mail: hirota-masatsugu@tsurumi-u.ac.jp

The purposes of this study were to evaluate the shear bond strength and perform the computational analysis for silane coupling treatments on the adhesion between CAD/CAM composite resin and resin cement. As silane coupling agents,  $\gamma$ -methacryloyloxypropyltrimethoxysilane, 8-methacryloyloxyoctyl trimethoxysilane, and 3-methacryloyloxypropyl trichlorosilane were used. The shear bond strengths were influenced by the silane coupling agent used, its application method, and acid addition. There was no correlation between the contact angle and shear bond strengths. The steric energy difference between a silane coupling agent and its corresponding hydrolyzed trisilanol compound,  $\Delta E$ , was calculated by the molecular mechanics method. There was a moderate or strong linear correlation between  $\Delta E$  and shear bond strengths in treatment without acid addition and a weak correlation between them in treatment with acid addition. Computational analysis could suggest the different path of silane coupling treatments of CAD/CAM composite resin in the presence or absence of acid.

**Keywords:** CAD/CAM resin, Resin cement, Silane coupling agents, Shear bond strength, Computational analysis

### INTRODUCTION

Advances in digital dentistry have led to remarkable progress in computer-aided design/computer-aided manufacturing (CAD/CAM) systems in dentistry<sup>1–4</sup>. In particular, composite resin crowns fabricated using CAD/CAM systems have been widely employed in dental clinical practice. As composite resin blocks for CAD/CAM system, fillers were filled with high density and resin matrixes were highly-cross linked<sup>5,6</sup>. It is well known that achieving adhesion with highly cross-linked resin is highly difficult. Thus, reliable bonding to CAD/CAM composite resin was attained by the bonding to highly filled inorganic fillers such as silica or alumina.

The shear bond strength between CAD/CAM composite resin and resin cement achieved with treatment using a silane coupling agent has been reported to be higher than that achieved without treatment<sup>7</sup>. Shinohara *et al.* reported that use of a silane coupling agent in combination with resin cement activated with a tributylborane derivative was effective in improving the bond strength of a CAD/CAM composite resin block<sup>8,9</sup>. The use of silane coupling agents has been recommended for achieving bonding between CAD/CAM composite resin and resin cement. Silane coupling agents are also widely used for porcelain bonding or repair of restorative composite resin<sup>10–12</sup>. The bonding of resin cement to porcelain is achieved through the formation of a siloxane bond between a silane coupling agent and a silica filler. Formation of such a siloxane bond between a silane coupling agent and a silica filler or porcelain is known to proceed *via* acid catalysis or heat treatment. Hayakawa *et al.* studied the influence of activation of  $\gamma$ -methacryloyloxypropyl trimethoxysilane ( $\gamma$ -MPTS) on bonding of restorative resins to porcelain and found that

the use of  $\gamma$ -MPTS ethanol solution in combination with acid with pH of 0.5–1.0 increased the bond strength of restorative resins to porcelain<sup>13</sup>.  $\gamma$ -MPTS is primarily used as a component of a majority of commercially available silane primers.

The mechanism of silane coupling agent treatment is highly complicated<sup>10,14,15</sup>. For example,  $\gamma$ -MPTS has trimethoxysilane groups. Treatment with  $\gamma$ -MPTS involves the following reactions: hydrolysis of the trimethoxysilane groups to the trisilanol groups, condensation of the trimethoxysilane or trisilanol groups to the hydroxyl groups of the silica surface, and condensation reactions among the trimethoxysilane or trisilanol groups<sup>10,15</sup>.

In the present study, first, the shear bond strength between CAD/CAM composite resin and resin cement was determined under different conditions of silane coupling treatment. Three kinds of silane coupling agents differing in terms of their concentration and presence or absence of an acid buffer were used. Next, the obtained shear bond strength data for the different silane coupling treatments were computationally analyzed in order to understand the mechanism of silane coupling treatment. Specifically, the steric energies of the silane coupling agents were calculated by the molecular mechanics (MM) method<sup>16,17</sup>. The computational analysis was able to suggest the mechanism of silane coupling treatment.

### MATERIALS AND METHODS

#### *Silane coupling agents*

$\gamma$ -MPTS (Shin-Etsu Chemical, Tokyo, Japan), 8-methacryloyloxyoctyl trimethoxysilane (MOTS; Shin-Etsu Chemical), and 3-methacryloyloxypropyl trichlorosilane (MPTCl; Sigma-Aldrich, St. Louis, MO,

USA) were used as silane coupling agents in this study. The structures of these silane coupling agents are shown in Fig. 1. Each silane coupling agent was dissolved in ethanol or acetone. The  $\gamma$ -MPTS and MOTS solutions were adjusted to a concentration of 1 or 2 wt% in ethanol. The MPTCl solution was also 1 or 2 wt% in acetone. KCl–HCl buffer solution (pH 1.0, Tokyo Chemical Industry,

Tokyo, Japan) was used as an acid buffer.

#### Procedure for measurement of shear bond strength

Details of the materials used in this study are listed in Table 1, and the procedure for measurement of the shear bond strength is depicted in Fig. 2.

A composite resin block for a CAD/CAM crown (hereafter referred to as “CAD/CAM resin block”; Katana Avencia Block, Kuraray Noritake Dental, Tokyo, Japan) was cut in the form of a plate with dimensions of 12.5×10.5×2.0 mm. Each plate was embedded in self-curing acrylic resin (Unifast III, GC, Tokyo, Japan). A flat surface of the CAD/CAM resin block was prepared *via* wet grinding with #600 emery paper under running water. Sandblasting was performed perpendicular to the surface from a distance of 20 mm with 50  $\mu$ m alumina particles at an air pressure of 0.4 MPa for 30 s. The block was then cleaned using an ultrasonic cleaner (VS-100 III, AS ONE, Osaka, Japan) in double-distilled water for 20 min. After drying of the block in a desiccator, an etching agent (K-etchant GEL, Kuraray Noritake Dental) was applied on the block surface for 5 s. Then, the etched surface was rinsed with double-distilled water for 10 s and was air dried for 5 s.

Afterwards, the surface of CAD/CAM resin block was treated separately with each silane coupling solution. The silane coupling treatment was performed by the following four procedures.

Procedure A: The block was treated with 1 wt% silane solution for 20 s and then washed with ethanol and dried *via* air blowing.

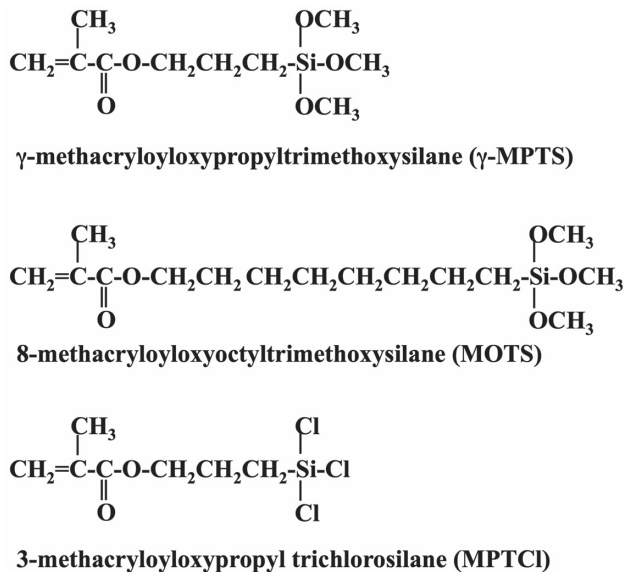


Fig. 1 Structural formulations of silane coupling agents.

Table 1 Details of materials used in this study

Material	Name	Lot no.	Manufacturer
CAD/CAM resin block	Katana Avencia Block	000167	Kuraray Noritake Dental, Tokyo, Japan
Resin cement	PANAVIA V5	9S0040	Kuraray Noritake Dental
Light-curing unit (LED)	Poly Wave	102286	Ivoclar Vivadent, Schaan, Liechtenstein
Etching agent	K-etchant GEL	AJ0046	Kuraray Noritake Dental
Metal adhesive primer	ALLOY PRIMER	6A0071	Kuraray Noritake Dental
Silane coupling agent	$\gamma$ -MPTS	607919	Shin-EtsuChemical, Tokyo, Japan
	MOTS	511003	Shin-EtsuChemical
	MPTCl	BCBM3883V	Sigma-Aldrich, St. Louis, MO, USA

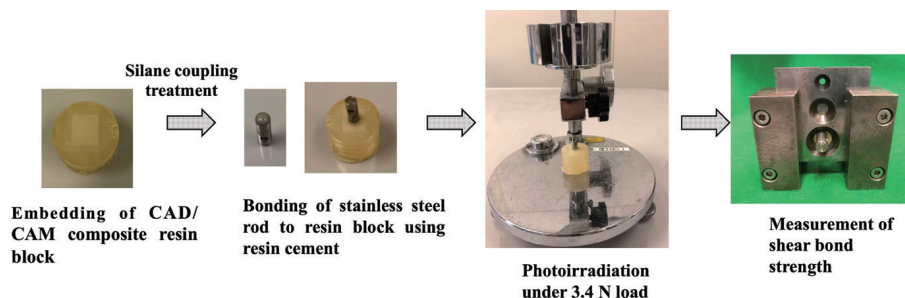


Fig. 2 Procedure for measurement of shear bond strength.

Procedure B: The block was treated with an equivalent mixture of 1 wt% silane solution and a pH=1 acid buffer for 20 s and then washed with ethanol and dried *via* air blowing.

Procedure C: The block was treated with 2 wt% silane solution for 20 s and then directly dried *via* air blowing without being washed with ethanol.

Procedure D: The block was treated with an equivalent mixture of 2 wt% silane solution and a pH=1 acid buffer for 20 s and then directly dried *via* air blowing without being washed with ethanol.

The surface of a stainless steel rod (6 mm in diameter and 15 mm in height) was sandblasted from a distance of 20 mm with 50  $\mu$ m alumina particles at an air pressure of 0.4 MPa for 30 s. After sandblasting, the stainless steel rod was cleaned using an ultrasonic cleaner in double-distilled water for 20 min and then treated with metal adhesive primer (ALLOY PRIMER, Kuraray Noritake Dental). A resin cement (PANAVIA V5, Kuraray Noritake Dental) was applied on the stainless steel rod. Then, the stainless steel rod with resin cement on top was pressed onto the surface of the silane-treated CAD/CAM resin block. Subsequently, a load of 350 g was applied to the stainless steel rod. The excess resin cement was removed using a dental explorer after light curing for 5 s by means of a light-emitting diode (LED) light-curing unit (Poly Wave, Ivoclar Vivadent, Schaan, Liechtenstein). Additionally, the resin cement between the stainless steel rod and the CAD/CAM resin block was light-cured for 20 s. The 350 g load was maintained for 10 min after photoirradiation. Test specimens were immersed in 37°C water for 1 day.

The shear bond strength was measured using a universal testing machine (Autograph AG-IS 20 kN, Shimadzu, Kyoto, Japan) at a crosshead speed of 1 mm/min. This measurement was performed according to the method of Noguchi and ISO/TS 11405:2015<sup>18,19</sup>. The number of test specimens for each condition was 8–12.

#### *Scanning electron microscopy observations of surfaces of CAD/CAM resin block and stainless steel rod before and after sandblasting*

The surface appearances of the CAD/CAM resin block and stainless steel rod before and after sandblasting were observed by scanning electron microscopy (SEM; JSM-5600LV, JEOL, Tokyo, Japan). The specimens were sputter-coated with Au and observed at an accelerating voltage of 15 kV.

#### *Electron probe microanalysis of CAD/CAM resin block surface*

Distributions of the silica filler of the CAD/CAM resin block after sandblasting were evaluated by electron probe microanalysis (EPMA; JXS-8900RL, JEOL) at an accelerating voltage of 15 kV through detection of the X-ray intensity of Si-K $\alpha$ . Si surface mapping was

performed.

#### *Contact angle measurement of CAD/CAM resin blocks after silane coupling treatment*

The surface wettability of the CAD/CAM resin blocks after treatment with each silane coupling agent was characterized by measurement of the contact angle with 0.5  $\mu$ L double-distilled water using an auto contact angle meter (DMe-201, Kyowa Interface Science, Saitama, Japan) with an attached analysis system (FAMAS, Kyowa Interface Science). Ten measurements for 3.0 s each were performed under each condition. All measurements were performed under the same conditions of room temperature (25 $\pm$ 1°C) and humidity (45 $\pm$ 1%).

#### *Steric energy calculation*

Steric energy calculations for the silane coupling agents were performed using a quantum chemistry CAChe software package (version 5.0, Fujitsu, Tokyo, Japan). CAChe, which was installed on a Microsoft Windows® 2000 operating system (WinBook WS series, SOTEC, Onkyo, Osaka, Japan), features accelerated color 3D-stereo computer graphics and various computational chemistry programs. In the present study, the steric energies of the silane coupling agents were calculated by the MM method<sup>16,17</sup>. MM models a molecule as if its atoms and bonds are interacting balls and springs by using equations from classical Newtonian physics. Empirically derived force fields describe bond stretching, bond angle bending, and non-bonded interactions such as van der Waals and hydrogen bond interactions. The sum of all these interactions is the amount of strain in the molecule. This is defined as steric energy of the molecules. Thus, MM calculation can optimize the molecule by systematically moving all atoms, until the net force acting on each atom is minimized. In this way, optimized geometry that corresponds to a steric energy minimum of the molecule is obtained by the MM calculation. Optimized geometry is the geometry which it the most stable confirmation of the molecule, and energy zero does not mean the most stable conformation. The steric energy obtained by MM method is different from heat of formation or activation energy. Heat of formation could be obtained by molecular orbital (MO) calculations<sup>20,21</sup>. MO calculation is based on the Schrödinger equation. It is impossible to perform MO calculation of silane coupling agents by our computer system due to too many electrons for calculations. The steric energy by MM method is available for comparison of the different conformations or configurations for the same molecule, but not the comparison between different molecules. For example, steric energy of methanol and ethanol obtained by MM2 method is 0.0609 and 0.8018 kcal/mol, respectively. It is impossible to determine that methanol is more stable than ethanol.

The steric energies of the three different silane coupling agents and their corresponding hydrolyzed trisilanols compounds were calculated. We assumed that  $\gamma$ -MPTS, MOTS and MPTCl will

hydrolyze to corresponding trisilanol compounds. The trimethoxysilane functional groups of  $\gamma$ -MPTS and MOTS will be hydrolyzed to the trisilanol group, and trichloro group of MPTCl will also be hydrolyzed to the trisilanol group. The chemical formulas of the hydrolyzed structures of the  $\gamma$ -MPTS and MOTS silane coupling agents are depicted in Fig. 3. The hydrolyzed

trisilanol compounds of these two silane coupling agents are hereafter referred to as  $\gamma$ -MPTS-OH and MOTS-OH, respectively. The structure of the hydrolyzed trisilanol compound of MPTCl was the same as that of  $\gamma$ -MPTS. Thus, hydrolyzed trisilanol compounds of MPTCl is also referred as  $\gamma$ -MPTS-OH. Then, the energy difference between the silane coupling agent and its corresponding hydrolyzed trisilanol compound,  $\Delta E$ , was calculated.

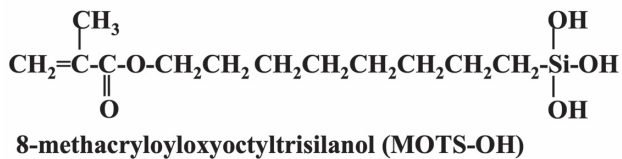
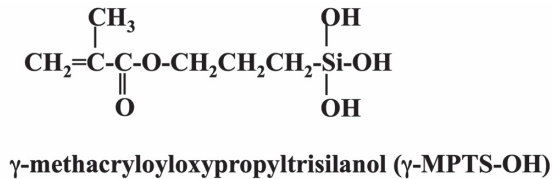


Fig. 3 Structural formulations of hydrolyzed compounds of silane coupling agents.

#### Statistical analysis

The measurement results of shear bond strength and contact angle were evaluated by a three-way analysis of variance (ANOVA) of the silane coupling agent (kinds of silane coupling agents, “Silane”), application method (*i.e.*, 1 wt% silane with washing *vs.* 2 wt% silane without washing, “Application method”), and application of acid treatment (with or without acid addition, “Acid”). Next, Tukey’s test for multiple comparisons was conducted to detect the significance among the four different procedures. Analysis was performed using Origin Pro 9.0 J (OriginLab, Northampton, MA, USA) with the mean at  $p=0.05$ .

## RESULT

The results of three-way ANOVA for the shear bond strength are presented in Table 2. Significant

Table 2 Results of three-way ANOVA for shear bond strength

Source of variation	DF	Sum of squares	Mean square	F-value	p-value
Silane	2	410.42521	205.21261	10.63635	<0.0001
Application method	1	59.94378	59.94378	3.10694	0.08093
Acid	1	267.61389	267.61389	13.87066	<0.001
Silane $\times$ Application method	2	219.22267	109.61133	5.68125	0.00457
Silane $\times$ Acid	2	465.0475	232.52375	12.05191	<0.0001
Application method $\times$ Acid	1	354.71138	354.71138	18.385	<0.0001
Silane $\times$ Application method $\times$ Acid	2	88.55914	44.27957	2.29505	0.10589
Model	11	2,173.76408	197.61492	10.24255	<0.0001
Error	103	1,987.23315	19.29353	0	0
Corrected Total	114	4,160.99723	0	0	0

Table 3 Results of measurement of shear bond strengths to silane-treated CAD/CAM resin blocks

Silane coupling agent	Procedure A (1 wt%)	Procedure B (1 wt%+pH=1 acid)	Procedure C (2 wt%)	Procedure D (2 wt%+pH=1 acid)
$\gamma$ -MPTS	5.7 (1.2) <sup>a</sup>	14.2 (4.4) <sup>b</sup>	15.7 (4.7) <sup>b</sup>	15.0 (2.3) <sup>b</sup>
MOTS	17.6 (3.0) <sup>c</sup>	16.3 (6.0) <sup>c</sup>	16.8 (5.3) <sup>c</sup>	13.5 (3.4) <sup>c</sup>
MPTCl	4.6 (3.3) <sup>d</sup>	17.5 (6.1) <sup>e,f</sup>	10.6 (3.9) <sup>e,g</sup>	13.2 (3.8) <sup>e</sup>

Values in parentheses denote the standard deviation (SD).

Superscripted letters indicate significant differences among the four kinds of surface treatment conditions with the same silane coupling agent ( $p<0.05$ ).



differences existed in Silane and Acid ( $p < 0.001$ ) but not in Application method ( $p > 0.05$ ). Significant interactions were observed between Silane and Application method, between Application method and Acid, and between Silane and Acid ( $p < 0.0001$ ). There was no three-way interaction among Silane, Application method, and Acid ( $p > 0.1$ ).

The results of measurement of shear bond strengths to the silane-treated CAD/CAM resin blocks are presented in Table 3. Computational analyses were performed using the measurement results of the shear bond strength between the CAD/CAM composite resin and resin cement under different silane coupling treatment conditions. Then, statistical analyses among the different procedures were performed for investigating the influence of differences in silane coupling treatment procedures on the shear bond strength.

In the case of treatment with  $\gamma$ -MPTS, procedure A (1 wt% with EtOH washing) yielded significantly lower bond strengths than procedures B, C, and D ( $p < 0.05$ ). There were no significant differences in the shear

bond strength among procedures B, C, and D ( $p > 0.05$ ). Treatment with the MOTS silane coupling agent did not lead to any significant differences in the shear bond strength among the four procedures ( $p > 0.05$ ). In the case of treatment with MPTC1, the shear bond strength achieved using procedure A was significantly lower than those achieved using procedures B, C, and D ( $p < 0.05$ ). No significant differences existed between procedures B and D and between procedures C and D ( $p > 0.05$ ).

SEM images of the surfaces of the CAD/CAM resin block and stainless steel rod before and after sandblasting are shown in Fig. 4. Before sandblasting, flat resin block surface were observed. Stainless rod showed many scratches by machining. Both the resin block and the rod were found to have roughened surfaces after sandblasting. No scratches on stainless rod surface

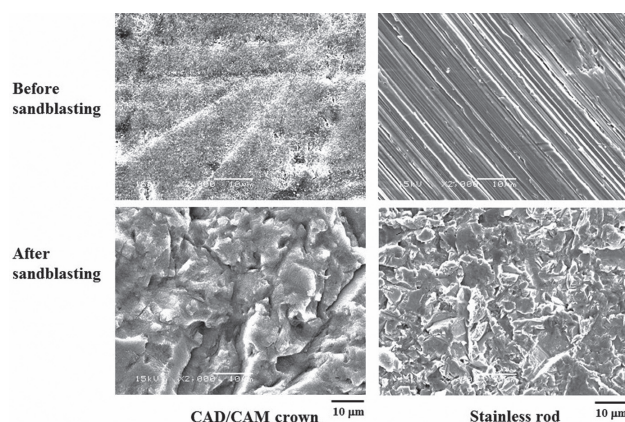


Fig. 4 SEM micrographs of surfaces of CAD/CAM composite resin and stainless steel rod.

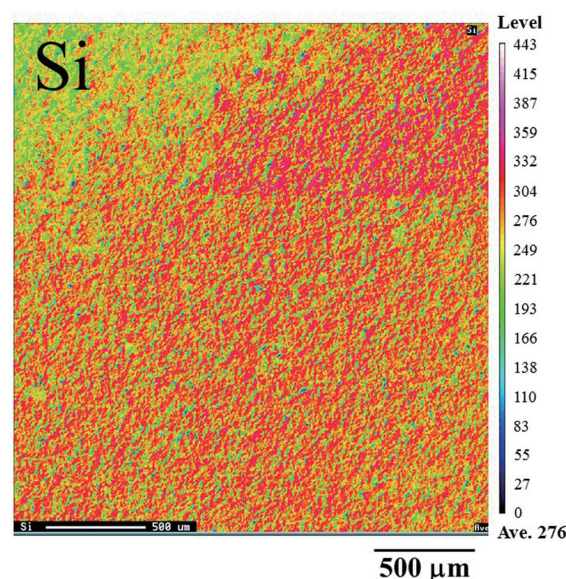


Fig. 5 EPMA analysis of surface of sandblasted CAD/CAM composite resin.

Table 4 Results of three-way ANOVA for contact angle

Source of variation	DF	Sum of squares	Mean square	F-value	p-value
Silane	2	1,323.87543	661.93771	14.31538	<0.00001
Application method	1	34,277.25338	34,277.25338	741.2964	0
Acid	1	808.77726	808.77726	17.49101	<0.0001
Silane $\times$ Application method	2	3,158.80109	1,579.40054	34.15688	<0.00001
Silane $\times$ Acid	2	2,611.41995	1,305.70998	28.23791	<0.00001
Application method $\times$ Acid	1	1,906.75383	1,906.75383	41.23638	<0.00001
Silane $\times$ Application method $\times$ Acid	2	1,844.54113	922.27056	19.94547	<0.00001
Model	11	51,434.15009	4,675.83183	101.12179	0
Error	128	5,918.66952	46.23961	0	0
Corrected Total	139	5,7352.8196	0	0	0

was found. Figure 5 shows the distribution of the Si element on the resin block surface as determined by EPMA analysis. Homogeneous distribution of Si of the compressed block of nano-sized silica fillers on the resin block surface was confirmed.

Table 4 lists the results of three-way ANOVA for the contact angle. Significant differences existed in Silane, Application method, and Acid ( $p < 0.0001$ ). Significant interactions were observed between Silane and Application method, between Application method and Acid, and between Silane and Acid ( $p < 0.0001$ ). There was a three-way interaction among Silane, Application method, and Acid ( $p < 0.0001$ ).

The results of measurement of the contact angle of the silane-treated resin block surface with double-distilled water are presented in Table 5. There were no significant differences between procedures A and B ( $p > 0.05$ ). Procedures C and D yielded significantly smaller contact angles than procedures A and B ( $p < 0.05$ ). No significant difference was detected between procedures C and D for  $\gamma$ -MPTS and MPTCl ( $p > 0.05$ ). Figure 6 shows the relationship between the contact angle and the shear bond strength between the CAD/CAD composite resin and resin cement. There was no correlation between the contact angle and the shear

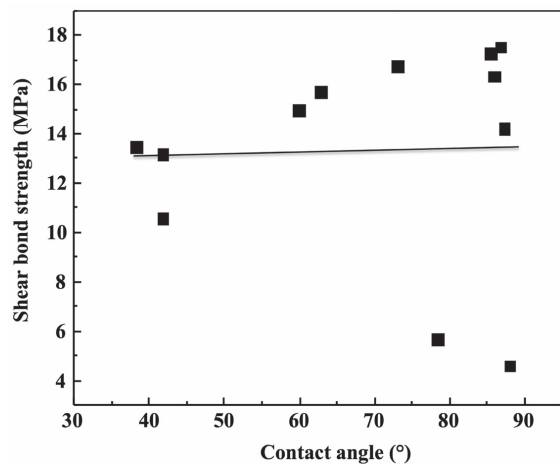


Fig. 6 Relationship of contact angle with shear bond strength between CAD/CAM composite resin and resin cement.

bond strength ( $r^2 < 0.001$ ).

The optimized geometries of each silane coupling agent and its corresponding hydrolyzed trisilanol compound as determined by the MM method are shown in Figs. 7–9.

$\gamma$ -MPTS and MPTCl had similar steric geometries and MOTS had a linear structure. Steric energies were calculated on the basis of the optimized geometries. Table 6 lists the steric energies of each silane coupling agent and its corresponding hydrolyzed trisilanol compound, as well as the respective  $\Delta E$  values. The steric energies of the silane coupling agents were in the following order: MOTS > MPTCl >  $\gamma$ -MPTS. The steric energy of the hydrolyzed trisilanol compound of MOTS was higher than those of MPTCl and  $\gamma$ -MPTS.

Figures 10–13 show the relationship between  $\Delta E$  and the shear bond strength in each procedure. There was a moderate linear correlation between  $\Delta E$  and the

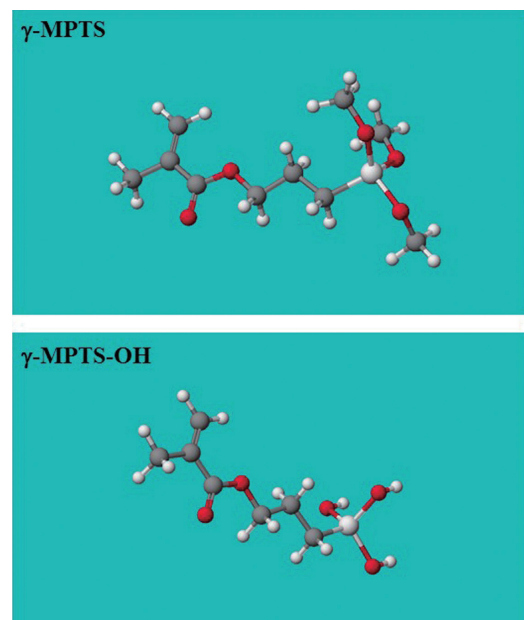


Fig. 7 Optimized structure of  $\gamma$ -MPTS and its hydrolyzed compound ( $\gamma$ -MPTS-OH). Dark gray: carbon, red: oxygen, blue: gray small: hydrogen, gray large: silicon

Table 5 Results of measurement of contact angles with silane-treated CAD/CAM resin blocks

Silane coupling agent	Procedure A (1 wt%)	Procedure B (1 wt%+pH=1 acid)	Procedure C (2 wt%)	Procedure D (2 wt%+pH=1 acid)
$\gamma$ -MPTS	78.4 (11.3) <sup>a</sup>	87.2 (4.5) <sup>a</sup>	62.8 (7.3) <sup>b</sup>	59.9 (9.1) <sup>b</sup>
MOTS	85.5 (5.9) <sup>a</sup>	85.9 (9.2) <sup>a</sup>	73.0 (1.9) <sup>b</sup>	38.2 (4.8) <sup>c</sup>
MPTCl	88.0 (8.6) <sup>a</sup>	86.7 (3.2) <sup>a</sup>	41.8 (4.2) <sup>b</sup>	41.8 (2.8) <sup>b</sup>

Values in parentheses denote the SD.

Superscripted letters indicate significant differences among the four kinds of surface treatment conditions with the same silane coupling agent ( $p < 0.05$ ).

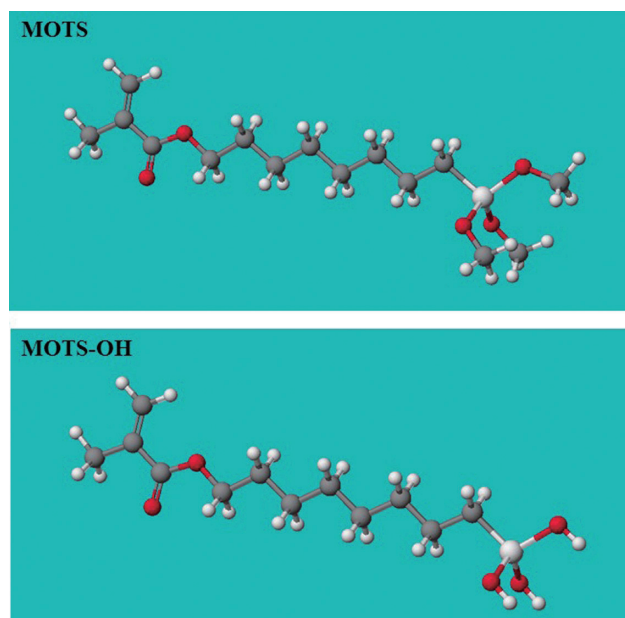


Fig. 8 Optimized structure of MOTS and its hydrolyzed compound (MOTS-OH).  
Dark gray: carbon, red: oxygen, blue: gray small: hydrogen, gray large: silicon

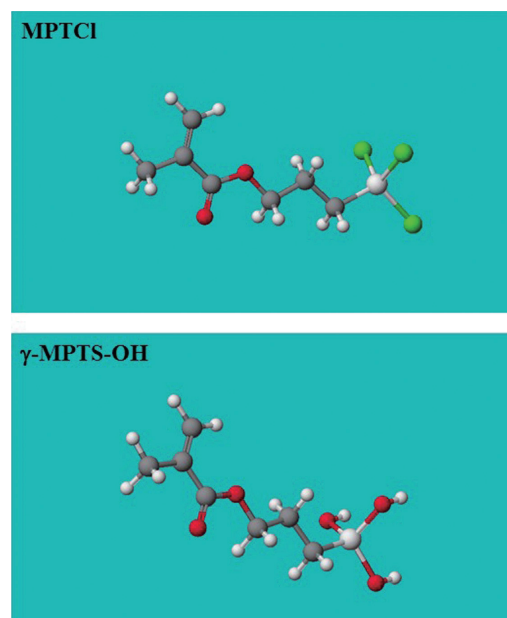


Fig. 9 Optimized structure of MPTCl and its hydrolyzed compound ( $\gamma$ -MPTS-OH).  
Dark gray: carbon, red: oxygen, blue: grey small: hydrogen, grey large: silicon

Table 6 Steric energies of silane coupling agents and their corresponding hydrolyzed trisilanol compounds and energy difference between silane coupling agent and its corresponding hydrolyzed trisilanol compound,  $\Delta E$

	Steric energy (kcal/mol)		$\Delta E$ (kcal/mol)
	Silane coupling agent	Corresponding hydrolyzed trisilanol compound	
$\gamma$ -MPTS	5.5699	-23.7308	29.3007
MOTS	10.6926	-17.0634	27.7560
MPTCl	8.0568	-23.7308	31.7876

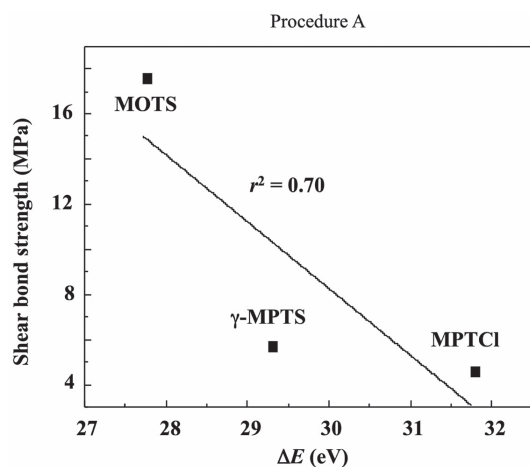


Fig. 10 Relationship between  $\Delta E$  (energy difference between silane coupling agent and its corresponding hydrolyzed trisilanol compound) and shear bond strength in procedure A.

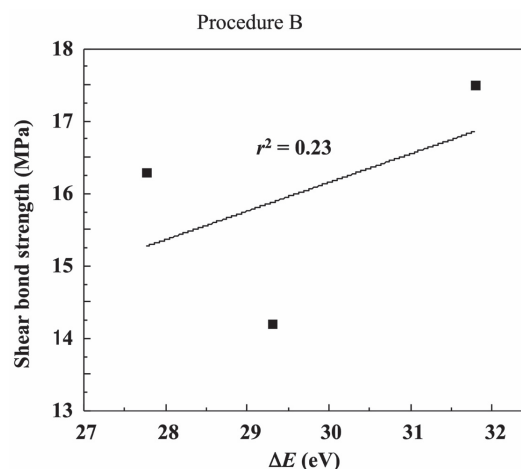


Fig. 11 Relationship between  $\Delta E$  (energy difference between silane coupling agent and its corresponding hydrolyzed trisilanol compound) and shear bond strength in procedure B.

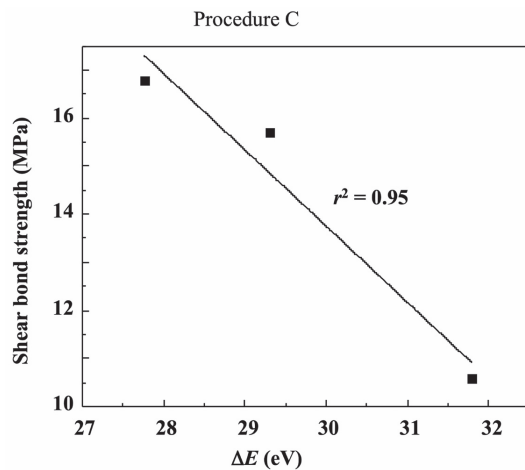


Fig. 12 Relationship between  $\Delta E$  (energy difference between silane coupling agent and its corresponding hydrolyzed trisilanol compound) and shear bond strength in procedure C.

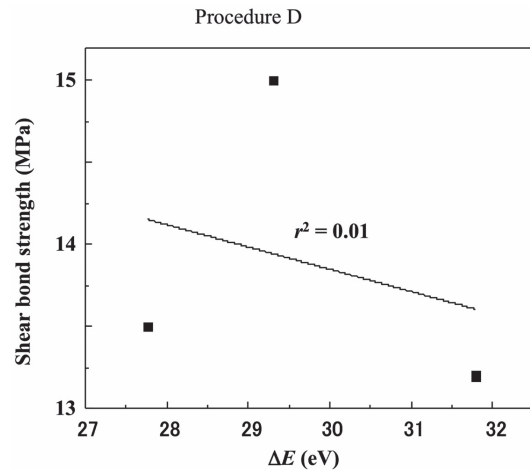


Fig. 13 Relationship between  $\Delta E$  (energy difference between silane coupling agent and its corresponding hydrolyzed trisilanol compound) and shear bond strength in procedure D.

shear bond strength in procedure A ( $r^2=0.70$ ) and a strong correlation between them in procedure C ( $r^2=0.95$ ), as shown in Figs. 10 and 12, respectively. On the contrary, there was a weak correlation between  $\Delta E$  and the shear bond strength in procedure B ( $r^2=0.23$ ) and a very weak correlation between them in procedure D ( $r^2=0.08$ ), as shown in Figs. 11 and 13, respectively.

## DISCUSSION

In the present study, we evaluated the shear bond strength between CAD/CAM composite resin and resin cement under different conditions of silane coupling treatment. We also analyzed the influence of different silane coupling treatments on the shear bond strength by a computational approach.

The stainless steel rod with resin cement was pressed on the surface of the CAD/CAM resin blocks as specimens for shear bond tests in this study. Thus, there are two interfaces between the stainless steel and resin cement, and between resin cement and CAD/CAM resin block. After the measurement of shear bond strength, cement layer was observed at the stainless steel rod surface. There was no residue of the resin cement on the CAD/CAM resin block surface. It means the bonding of resin cement to stainless steel rod treated with metal adhesive primer was superior to that to silane treated CAD/CAM resin block.

Katana Avencia Block was prepared by monomer infiltration method<sup>22</sup>. Namely, resin monomer was uniformly impregnated into the compressed block of nano-sized silica fillers. EPMA analysis revealed the homogeneous distribution of nano-sized silica fillers. CAD/CAM resin block with more densely packed nano-sized filler can be fabricated by using monomer infiltration method. It is reported that the content of nano-sized silica filler was up to 70%<sup>22</sup>.

In our study,  $\gamma$ -MPTS, MOTS, and MPTCl were used as silane coupling agents. Maruo *et al.* investigated the efficacy of MOTS treatment for bonding resin cement to lithium disilicate glass<sup>23</sup>. Koh *et al.* reported the use of MPTCl for the silanization of silicon and glass surfaces<sup>24</sup>. MOTS has a longer methylene chain than  $\gamma$ -MPTS and the same trimethoxysilane structure as  $\gamma$ -MPTS. On the contrary, the length of the methylene chain of MPTCl is identical to that of  $\gamma$ -MPTS and the trimethoxysilane structure of MPTCl is different from that of  $\gamma$ -MPTS.

In the present study, we tested two different concentrations of the silane coupling agent —1 and 2 wt%. In the case of 1 wt% silane coupling agent treatment, ethanol washing was employed. Ethanol washing will remove the physiological adsorbed silane coupling agents and will form monolayer of silane coupling agents. Thus, it will be possible to investigate the influence of different adsorbed structures of silane coupling agents, monolayer or multilayer on the bond strength to CAD/CAM resin with or without ethanol washing. We conjectured the silane coupling layer on the CAD/CAM resin surface to be as shown in Fig. 14. Namely, we speculated that treatment with a 1 wt% silane coupling agent and subsequent ethanol washing (procedures A and B) would result in the formation of a monolayer of the silane coupling agent on the CAD/CAM resin surface and that treatment with a 2 wt% silane coupling agent without subsequent ethanol washing (procedures C and D) would result in the formation of a multilayer of the silane coupling agent on the CAD/CAM resin surface. It was thought that the monolayer and multilayer structures of the silane coupling agent would have different influences on the shear bond strength. However, only significant differences were observed between procedures A and C in the cases of  $\gamma$ -MPTS and MPTCl treatments. MOTS has a longer methylene chain. Thus, the steric hindrance of MOTS was expected



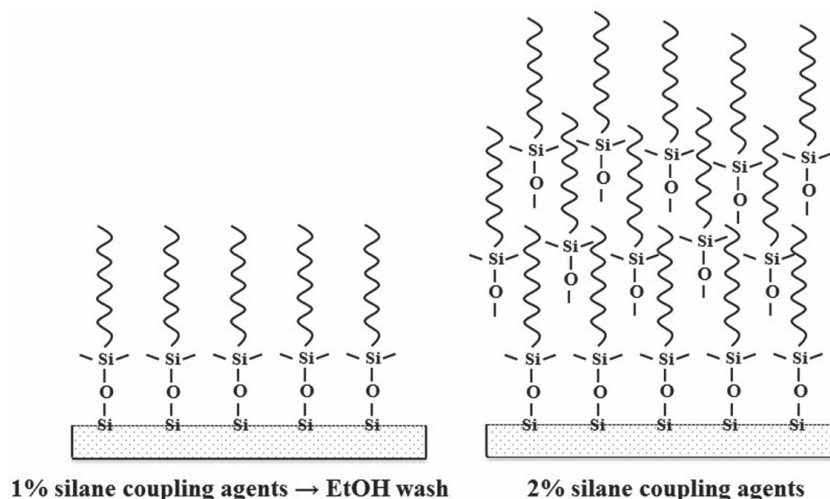


Fig. 14 Schematic diagrams of monolayer and multilayer of silane coupling agents.

to influence the type of silane coupling layer formed (*i.e.*, monolayer or multilayer). Maruo *et al.* stated the longer hydrocarbon chain of silane coupling agents influenced the self-condensation reaction of silane coupling agents<sup>23)</sup>. Moreover, the decrease in the water contact angles for 2 wt% application of MOTS and MPTCl was observed. The reason for the decrease in the water contact angles was not clear. But it is presumed that the differences in the structure of multilayer formation, namely packing conditions, thickness, orientation of silane coupling agents etc, may influence the contact angles. Detailed surface analysis of silane coupling layers is required for further examination of this hypothesis.

In this study, we adopted the computational approach of calculating the steric energies of each silane coupling agent and its corresponding hydrolyzed trisilanol compound by the MM method. Hayakawa *et al.* reported a conformational analysis of dental adhesive monomers by the MM method<sup>21)</sup>. Hayakawa *et al.* also analyzed the reactivity of bisphosphonate compounds toward Ca ions by the MM method<sup>25)</sup>. They found that the energy difference between the bisphosphonate/Ca complex and bisphosphonate was correlated with the reactivity of bisphosphonate toward Ca ions.

As mentioned above, the mechanism of silane coupling agent treatment is highly complicated. Some reported the direct condensation of silane coupling agents with OH group of silica to form Si-O-Si bonds without any requirement of prehydrolysis<sup>26,28)</sup>. In order to consider the mechanism of silane coupling treatments by computational approach, we simply presumed that the formation of a siloxane bond by the silane coupling agents occurred according to either of these paths, path a) and path b), as shown in Fig. 15. More complex processes were eliminated. In path a), hydrolysis of the trimethoxysilane or trichlorosilane group occurred and the condensation reaction of the trisilanol group to the silica hydroxyl group proceeded. In path b), the siloxane

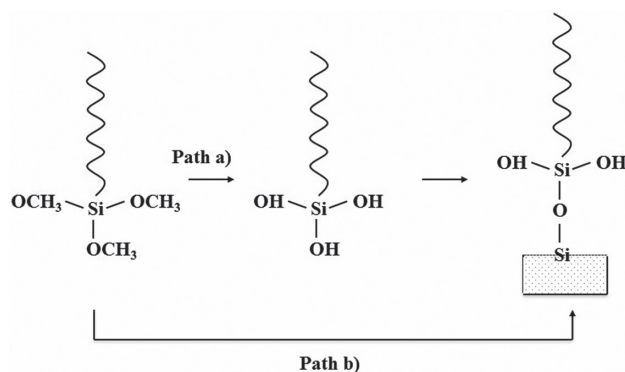


Fig. 15 Two different paths of siloxane bond formation. a): path involving hydrolysis and condensation reaction, b): path involving direct condensation.

bond was directly formed by the condensation reaction between the trimethoxysilane or trichlorosilane group and the silica hydroxyl group.

In procedures A and B, there was a linear correlation between  $\Delta E$ , which is the energy difference between a silane coupling agent and its corresponding hydrolyzed trisilanol compound, and the shear bond strength.  $\Delta E$  is the difference of steric energies between each silane coupling agents and their corresponding hydrolyzed compounds with most stable conformation. Although there are many factors for affecting the hydrolysis reaction of each silane coupling agent, we employed  $\Delta E$  as one of the parameter for influencing the hydrolysis reaction. We simply assumed as following, namely, smaller  $\Delta E$  means that energy barrier for the change of silane coupling agents to its hydrolyzed compound will be smaller and corresponds to easier formation of the trisilanol compound. We searched the relationship between  $\Delta E$  and shear bond strength in each procedure. Thus, the formation of the trisilanol compound may contribute to the mechanism of silane coupling treatment.

It is speculated that path a) was dominant in procedures A and C. On the contrary, in procedures B and D, there was no correlation between  $\Delta E$  and the shear bond strength. The formation of the trisilanol compound had less contribution to the mechanism of silane coupling treatment in procedures B and D, and path b) was dominant in these two procedures. Acid activation promoted the direct condensation reaction between the trimethoxysilane or trichlorosilane group and the silica hydroxyl group, which resulted in the formation of the siloxane bond. Our adopted computational approach involving the MM method can explain the different path of silane coupling treatments in the presence or absence of acid.

However, MM method cannot predict the whole reaction process of molecules. MO calculation can give more information for the reactivity of each molecule such as orbital energies, electron densities or dipole moments *etc.*<sup>21)</sup>. But our computer system cannot calculate silane coupling agents due to too many electrons as described above. Thus, we compared the hydrolysis reaction by using MM method. There are many factor for affecting the hydrolysis of silane coupling agents. Our assumption is just simple and primitive. But we intended such simple and primitive assumption can gave some information for hydrolysis reaction of silane coupling agents. More detailed study for reactivity or reaction process of silane coupling agents should be performed by MO calculation or other advanced quantum chemical calculation such as density functional theory<sup>29)</sup>.

Actually, silane coupling agent treatment is influenced by many factors such as concentration of silane coupling agents, application conditions of silane coupling agents, pH of acid catalysis, kinds of silica filler, reactivity toward the silica surface or reactivity of OH groups of silica surface *etc.* The influence of these factors on the shear bond strengths of CAD/CAM resin block should be examined further as the next step in our research.

In the present study, addition of acid to the silane coupling agent did not necessarily improve the shear bond strength. It is presumed that acid activation promoted not only the condensation reaction of the trimethoxysilane or trisilanol group to the hydroxyl group of the silica surface but also the condensation reaction among the molecules of the silane coupling agent. Furthermore, not all the silane coupling treatments yielded a hydrophobic CAD/CAM resin surface.

## CONCLUSIONS

In this study, the shear bond strength for silane coupling treatments on the adhesion between CAD/CAM composite resin and resin cement was evaluated and the computational analysis for considering the mechanism of silane coupling treatment was performed. The shear bond strengths were influenced by the silane coupling agent used, its application method, and acid addition. There was no correlation between the contact angle and the shear bond strengths. As a computational approach,

steric energy difference between a silane coupling agent and its corresponding hydrolyzed trisilanol compound,  $\Delta E$ , was calculated by the MM method. There was a moderate or strong linear correlation between  $\Delta E$  and shear bond strengths in treatment without acid addition and a weak correlation between them in treatment with acid addition. Our simple computational approach could suggest the different path of silane coupling treatments of CAD/CAM composite resin in the presence or absence of acid.

## REFERENCES

- 1) Beuer F, Schweiger J, Edelhoff D. Digital dentistry: an overview of recent developments for CAD/CAM generated restorations. *Br Dent J* 2008; 204: 505-511.
- 2) Miyazaki T, Hotta Y, Kunii J, Kuriyama S, Tamaki Y. A review of dental CAD/CAM: current status and future perspectives from 20 years of experience. *Dent Mater J* 2009; 28: 44-56.
- 3) Van Noort R. The future of dental devices is digital. *Dent Mater* 2012; 28: 3-12.
- 4) Alghazzawi TF. Advancements in CAD/CAM technology: options for practical implementation. *J Prosthodont Res* 2016; 60: 72-84.
- 5) Ruse ND, Sadoun MJ. Resin-composite blocks for dental CAD/CAM applications. *J Dent Res* 2014; 93: 1232-1234.
- 6) Awada A, Nathanson D. Mechanical properties of resin-ceramic CAD/CAM restorative materials. *J Prosthet Dent* 2015; 114: 587-593.
- 7) Yoshida K, Kamada K, Atsuta M. Effects of two silane coupling agents, a bonding agent, and thermal cycling on the bond strength of a CAD/CAM composite material cemented with two resin luting agents. *J Prosthet Dent* 2001; 85: 184-189.
- 8) Shinohara A, Taira Y, Sawase T. Effects of tributylborane-activated adhesive and two silane agents on bonding computer-aided design and manufacturing (CAD/CAM) resin composite. *Odontology* 2017; 105: 437-442.
- 9) Shinohara A, Taira Y, Sakihara M, Sawase T. Effects of three silane primers and five adhesive agents on the bond strength of composite material for a computer-aided design and manufacturing system. *J Appl Oral Sci* 2018; 26: e20170342.
- 10) Lung CYK, Matinlinna JK. Aspects of silane coupling agents and surface conditioning in dentistry: an overview. *Dent Mater* 2012; 28: 467-477.
- 11) Nihei T. Dental application for silane coupling agents. *J Oral Sci* 2016; 58: 151-155.
- 12) Matinlinna JP, Lung CYK, Tsoi JKH. Silane adhesion mechanism in dental applications and surface treatments: a review. *Dent Mater* 2018; 34: 13-28.
- 13) Hayakawa T, Horie K, Aida M, Kanaya H, Murata Y. The study on the activation of the silane coupling agent. I. The effect of phosphoric acid aqueous solutions with various pH. *Adhes Dent* 1991; 9: 164-169.
- 14) Brzoska JB, Azouz IB, Rondelez F. Silanization of solid substrates: a step toward reproducibility. *Langmuir* 1994; 10: 4367-4373.
- 15) Yoshihara K, Nagaoka N, Sonod A, Maruo Y, Makita Y, Okihara T, *et al.* Effectiveness and stability of silane coupling agent incorporated in 'universal' adhesives. *Dent Mater* 2016; 32: 1218-1225.
- 16) Osawa E, Musso H. Application of potential-energy calculations to organic chemistry. Part 15. Molecular-mechanics calculations nonquatum-mechanical model. *Angew Chem* 1983; 95: 1-12.
- 17) Komeiji Y, Tajima S, Haraguchi M, Takahashi N, Uebayasi

- M, Nagashima U. Molecular dynamics simulation of biological molecules (2) Practice. *J Chem Software* 2001; 7: 1-28.
- 18) Noguchi N, Nakamura K, Ozone Y, Etchu Y. On adhesive and mechanical properties of dental cements—thermal influence. *Jpn J Dent Mater* 1985; 4: 543-550.
- 19) ISO/TS 11405:2015 Dentistry —Testing of adhesion to tooth structure. International Organization for Standardization.
- 20) Hirota M. Application of molecular orbital theory to organic chemistry. Sendai, Shokabo Co., Ltd. 1999. ISBN 978-4-7853-3207-5
- 21) Hayakawa T, Kikutake K, Nemoto K. Conformational and quantum analysis of dental adhesive carboxylic acid and carboxylic acid anhydride monomers. *Dent Mater J* 2001; 20: 1-15.
- 22) Okada K, Kameya T, Ishino H, Hayakawa T. A novel technique for preparing dental CAD/CAM composite resin blocks using the filler press and monomer infiltration method. *Dent Mater J* 2014; 33: 203-209.
- 23) Maruo Y, Nishigawa G, Yoshihara K, Minagi S, Matsumoto T, Irie M. Does 8-methacryloxyoctyl trimethoxy silane (8-MOTS) improve initial bond strength on lithium disilicate glass ceramic? *Dent Mater* 2017; 33: e95-e100.
- 24) Koh WG, Revzin A, Simonian A, Reeves T, Pishko M. Control of mammalian cell and bacteria adhesion on substrates micropatterned with poly (ethylene glycol) hydrogels. *Biomed Microdevices* 2003; 5: 11-19.
- 25) Hayakawa T, Furuya N, Yasuoka S, Katoh T, Fukushima T. Computational analysis of bisphosphonates and bisphosphonate/calcium complexes. *J Oral Tissue Engin* 2010; 8: 107-114.
- 26) Alexander Y, Fadeev AF, McCarthy TJ. Trialkylsilane monolayers covalently attached to silicon surfaces: wettability studies indicating that molecular topography contributes to contact angle hysteresis. *Langmuir* 1999; 15: 3759-3766.
- 27) Krasnoslobodtsev AV, Smirnov SN. Effect of water on silanization of Silica by trimethoxysilanes. *Langmuir* 2002; 18: 3181-3184.
- 28) Xie Y, Hill CAS, Xiao Z, Militz H, Mai C. Silane coupling agents used for natural fiber/polymer composites: A review. *Compos Pt A-Appl Sci Manuf*. 2010; 41: 806-819.
- 29) Elkin M, Newhouse TR. Computational chemistry strategies in natural product synthesis. *Chem Soc Rev* 2018; 47: 7830-7844.